

Krystyna Wrześniewska-Tosik^{1,*},
Ewa Wesołowska¹,
Joanna Ryszkowska²,
Sarah Montes³,
Tomasz Mik¹,
Tomasz Kowalewski¹,
Michał Kudra¹

Evaluation of the Thermal Stability of Keratin Fibres as a Component of Spun-Bonded Nonwovens for the Manufacture of Thermoset Bio-based Composites

DOI: 10.5604/01.3001.0013.1827

¹ ŁUKASIEWICZ Research Network
– Institute of Biopolymers and Chemical Fibres,
ul. M. Skłodowskiej-Curie 19/27,
90-570 Łódź, Poland
* e-mail: protein@ibwch.lodz.pl

² Warsaw University of Technology,
Faculty of Materials Engineering,
ul. Wołoska 141
02-507 Warszawa, Poland

³ CIDETEC,
Parque Tecnológico de Miramon,
20014 Donostia – San Sebastian, Spain

Abstract

The possibility of using animal wastes in the form of feathers for the production of various types of composites is an extremely original concept, opening to researchers a wide field for experiments and interdisciplinary scientific research. This article presents the results of studies on the thermal stability of keratin from feathers originating from various poultry slaughterhouses, as well as an example of the use of feathers for the production of thermosetting composites. The keratin protein contained in feathers, like any protein, is very sensitive to various external factors, e.g. high temperature. The scientific goal of the research presented in the article was a deep analysis of changes occurring in the structure of keratin protein in feathers during heating. The technological goal was to develop new thermosetting composites based on spun-bonded nonwovens with the addition of keratin fibres from poultry feather wastes.

Key words: keratin fibres, PP nonwoven, PLA nonwoven, feathers, spun-bonded technique, thermoset composites, thermal analysis.

Introduction

Environmental protection, economic pressure, as well as the need of reducing the dependence on non-renewable resources of crude oil have increased interest in the use of biomass as a renewable and sustainable source of raw materials. Poultry feathers, a rich source of keratin protein, have become an attractive raw material for the manufacture of bio-derived products.

The possibility of application of such a waste of animal origin in the form of feathers for the manufacture of various types of composites is an extremely original concept, opening up for researchers a wide field for experiments and interdisciplinary scientific research.

This article presents the results of thermal stability studies of keratin from feathers derived from different poultry

slaughterhouses as well as an example of the use of feathers for the manufacturing of thermoset composites. The keratin protein included in feathers, like any protein, is very sensitive to various external factors, e.g. high temperature.

The scientific objective of the research presented in the article was a deep analysis of changes occurring in the structure of keratin protein in feathers during heating.

The technological objective was to develop new thermoset composites based on spun-bonded non-woven with the addition of keratin fibres from poultry feathers and bio-based resins.

Forming nonwovens by the spun-bonded method takes place at the flow temperature of the base polymer – Polypropylene and Polylactic acid, i.e. 190 and 210 °C, respectively. Therefore, the results of the temperature impact on keratin obtained are crucial for the manufacturing of nonwovens containing feathers.

Experimental

Materials use

The following materials were used for the assessment of the thermal behaviour of feathers and for the manufacture of the thermoset composites.

- Six samples of feathers were selected for the tests, a description of which is summarised in **Table 1**.
- Polypropylene (PP HP648T, Brenntag Sp.zo.o, Poland; MFR: 49 g/10 min).
- Polylactide (PLA 6202D, Ingeo™, NatureWorks LLC, USA; MFR: 15-30 g/10 min).
- Epoxy resin (Super Sap® CLR, Entropy resins).

Methodology

Fragmentation of feathers

Cleaned, wet feathers were shredded in the following stages:

- by the grinding of wet feathers using an industrial shredder (fragments of ~5-10 mm),
- by the grinding of dried feathers in a planetary ball mill (XQM-16A) into smaller fragments. The milling process was carried out at a speed of 300 rpm for 12 hours,
- by separation according to size on a vibratory sieve shaker type AS 450 (Retsch), equipped with meshes of 250, 125, 63, 45 and 25 µm size. The smallest fraction (25 µm) was ad-

Table 1. Feather analysis.

Sample number	Name of sample/ Producer	Fat content, %	N content, %	C content, %	S content, %	Ash content, %
1	Szynkielew/Poland	3.45	12.39	50.07	1.84	0.79
2	Cedrob/Poland	3.07	15.39	47.75	2.71	0.75
3	Sada 6-9/Spain	3.25	15.50	51.80	2.35	0.80
4	Sada 9/Spain	7.45	15.83	52.55	2.52	0.76
5	Vive/Poland	1.25	12.55	39.77	2.51	0.60
6	Sada 9-25/Spain	4.36	15.29	53.44	2.46	0.99

ditionally sieved on a mesh of 10 μm size. Sieving for all trials was performed for 60 min at 2 mm amplitude.

Preparation of nonwoven based on polypropylene (PP), polylactide (PLA), polypropylene/chicken feathers (PP/CF) and polylactide/chicken feathers (PLA/CF)

PP and PLA based nonwovens with and without feathers were prepared at IBWCh by the spun-bonded technique described in Patent PL 230434 (2018.10.31) “Manufacture of a composite nonwoven”; however, the method for incorporation of feathers was different for PP (i) and PLA (ii) due to the need to adjust the appropriate conditions of the manufacturing process to achieve intended properties of the target products.

(i) The manufacture of PP/CF nonwoven aimed to develop non-woven materials with flame retardant properties by the introduction of a fireproof agent in the form of feather particles to the Polypropylene structure. The manufacture of PP/CF spun-bonded non-woven fabric with reduced flammability consisted of the following stages:

- feather preparation based on preliminary fragmentation in an industrial shredder and thorough grinding in a planetary-ball mill, which was then sorted in order to obtain the required form of feathers, with a particle size of about 5 μm ,
- raw material preparation consisting in the mixing of polymer granulate (PP) with ground feathers in appropriate proportions in order to coat the polymer granules with “keratin dust” (so-called powdering),
- drying the mixture to remove residual water associated with ground feathers (water disrupts the fibre formation process),
- forming, which is the manufacture of spun-bonded non-woven from a polymer blend (PP + feathers) and calendaring at a temperature of 130 $^{\circ}\text{C}$.

The PP/CF nonwoven contained 4% feathers i.e. the minimum quantity of feathers which ensures flame retardant properties of the nonwoven.

(ii) For PLA targeted products, the goal was to develop fully bio-based non-woven materials by the combination of two fully bio-based materials – PLA and feathers as well as to utilize feathers in quantities that maximise the lev-

el of renewable primary raw materials. The manufacture of PLA/CF spun-bonded non-woven consisted of the following stages:

- preliminary fragmentation in an industrial shredder in order to obtain feathers with a particle size of about 10 mm,
- processing of the molten polymer, where PLA was passed through a spinner, and then the fibres were stretched and cooled with air. The cooling air sucked the air stream with particles of feathers. The stretched polymer fibres together with the particles of shredded feathers, after passing through the forming channel, fell into a transport sieve in the form of a fleece. Then the pre-laminated fleece was calendered at a temperature of 90 $^{\circ}\text{C}$.

The PLA/CF nonwoven obtained contained 43% feathers.

Preparation of thermosetting composites (KMC) based on epoxy resins and spun-bonded non-woven fabrics

Composites were manufactured at CI-DETEC, Spain, by the combination of a bio-based epoxy resin (Super Sap® CLR, Entropy resins) and five layers of non-woven fabric. For this purpose, five layers of non-woven fabrics were impregnated with a mixture of resin and hardener (ratio 2:1) at room temperature, and the whole system was placed in a vacuum system and kept in an oven for 3 hours at 80 $^{\circ}\text{C}$ for curing.

This procedure was used for preparation of the following composites: PP and PLA based non-woven with and without CF (Table 2).

Analytical and testing methods

Ash content

The overall content of ash in the feathers (expressed in %) was analysed according to: ISO 936: 2000.

Content of C elemental

The content of carbon in feathers (expressed in % of the elemental carbon) was established according to NLS30/16 edition 1 dated 2016-12-05, with the use of an Elemental Macro cube analyser.

Content of N elemental

The content of nitrogen in feathers (expressed in % of the elemental nitrogen), examination made according to

Table 2. Bio-based composites prepared with non-woven fabrics. Note: *5 layers in all composites.

Thermoset composite	Non-woven*
KMC-1	PP
KMC-2	PP + 4%CF
KMC-3	PLA
KMC-4	PLA + 43%CF

NLS30/16 edition 1 dated 2016-12-05 with the use of the analyzer Elemental Macro cube.

Content of S elemental

The content of sulfur in feathers (expressed in % of the elemental sulfur) was analysed according to NLS30/16 edition 1 dated 2016-12-05, with the use of an Elemental Macro cube analyser.

Determination of fat content in poultry feathers

Fat from the feathers was removed by extraction with ethyl alcohol. 10 g of dry feathers were milled in a Körner mill, extracted with ethyl alcohol on Soxhlet apparatus for 3 h, and then dried at ambient temperature. The fats extracted were dried in a dryer with forced air circulation for 1 h, and then in an oven with infrared radiators at 105 $^{\circ}\text{C}$ until constant weight (4 h).

Infrared spectroscopy

Fourier transform infrared spectroscopy (FTIR) was performed using Nicolet FT-IR 6700 apparatus (ThermoElectrone Corporation, USA). Spectra were recorded in the range from 400 to 4000 cm^{-1} , at a resolution of 4 cm^{-1} , over 64 scans. Data analysis was performed using Omnic software. A baseline correction with CO_2 and H_2O was made to eliminate the impact of the compound’s residues from the feathers’ treatment.

Thermal analysis – TGA and DSC

Thermal stability of the feathers was assessed by thermogravimetric analysis (TGA) using a TA Instruments TGA Q500 (USA). The samples tested, weighing approx. 5 mg, were heated from room temperature to 250 $^{\circ}\text{C}$ at a rate of 10 $^{\circ}\text{C}/\text{min}$. The tests were carried out in an air atmosphere at a flow rate of 90 ml/min.

DSC measurements were performed using a differential scanning calorimeter – DSC Q1000 (TA Instruments, USA). Feathers were placed in hermetic aluminum pans and heated at the rate of 10 $^{\circ}\text{C}/\text{min}$ in the temperature range -90 $^{\circ}\text{C}$ to 220 $^{\circ}\text{C}$.

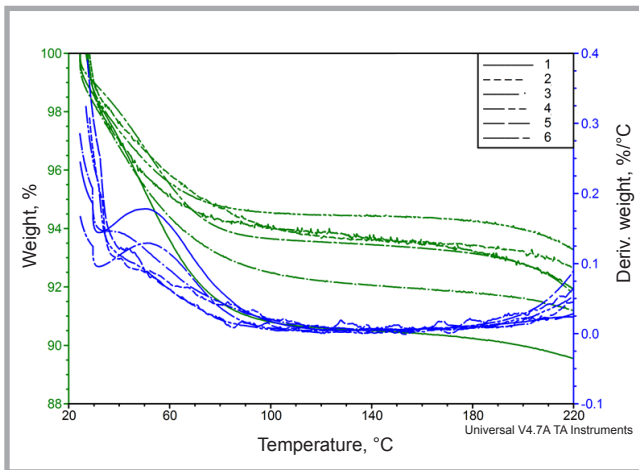


Figure 1. TGA and DTG thermograms of feathers.

carbonyl group of one amino acid and the amide group of the other. The β -sheet structure is characterised by inter-chain hydrogen bonds between the amide and carbonyl groups in the protein backbone [1]. The hydrogen bond can be combined with water bound in the protein structure. Keratin is characterised by high stability due to the inter-molecular bonding between polar and non-polar amino acids and poor solubility due to the presence of S-S bonds between cysteine- amino acids [2].

Thermal resistance of the feather samples was analysed from the mass change and curve of differential mass change using TGA analysis (**Figure 1**).

The first peak related to mass change is observed at 25-125 °C, with a mass loss of about 6-10%. In the range of 125-150 °C, the mass of the feather samples changes insignificantly, but above this temperature the weight loss rate of the samples increases. The interpretation of phenomena occurring during the heating of feathers is difficult, therefore **Figures 2** and **3** present an example interpretation of TGA curves in the context of DSC results for selected feather samples.

On the TGA curves the first stage of mass loss in the range of 25-70 °C (between T_1 and T_2) is observed, which is related to the evaporation of water [3]. The temperature at which this step ends may depend on the fat content covering the surface of the keratin fibres.

For some materials, the temperature of the end of the first step of water release is not marked.

Analysis of gases separated during heating of feathers

Analysis of gases separated during the heating of feathers in an air atmosphere was made using the TGA/FTIR method. Feathers were heated from room temperature to 300 °C at a rate of 20 °C/min. The gas cell FTIR was kept at 250 °C, and the temperature of the transmission line was set at 240 °C in order to reduce the possibility of evolving products condensing along the transmission line.

FE-SEM

The morphology of cross-sections of the biocomposites was analysed using an ULTRA plus ZEISS field emission scanning electron microscope (CIDETEC). Composite samples were cryogenically fractured and coated by sputter coating to apply an ultra-thin coating of gold (electrically-conducting metal). The coating of samples is required in the field of electron microscopy to enable the imaging of samples. Sputtering was carried out on a BAL-TEC SCD 005 sputter coater, with a current of 65 mA for 12 s.

Mechanical characterisation

Composites were mechanically characterised using a Universal testing machine (Instron, model 3365). Rectangular test specimens (65 mm x 12 mm) with a crosshead speed of 10 mm min⁻¹ and initial gauge length of 25.4 mm were used. The average tensile strength, elongation at break and Young's modulus were calculated from the resulting stress-strain curves. The measurements were made at room temperature and at least ten samples tested (CIDETEC).

Results and discussion

Structure of keratin feather fibres

Molecules of keratin proteins form different types of structures: α -helix, β -sheets or a random macrostructure. Keratin feather fibre consists of 41% α -helix, 38% β -sheets and 21% disordered conformation [1].

In the α -helix structure there are intra-molecular hydrogen bonds between the

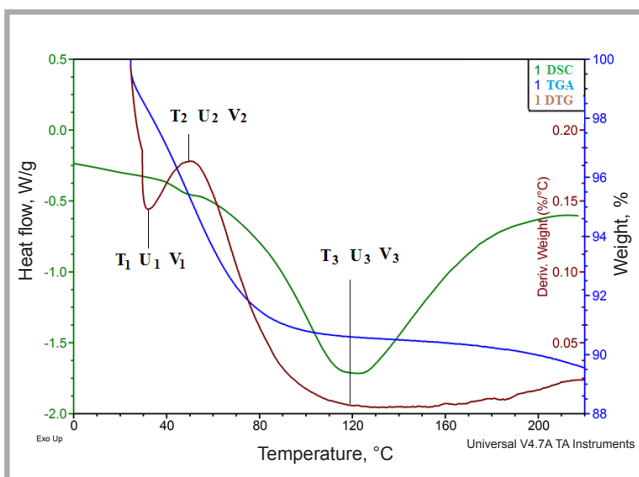


Figure 2. Interpretation of TGA curves in the context of changes in DSC thermograms (sample 1).

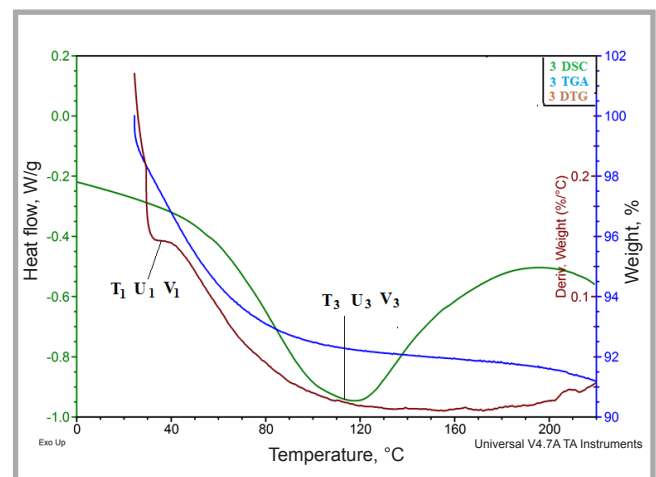


Figure 3. Interpretation of TGA curves in the context of changes in DSC thermograms (sample 3).

Table 3. Thermal characteristics of feathers at temperatures below 180 °C using TGA. **Note:** *total weight loss after the next step.

Sample number	T _{2%} , °C	T ₁ , °C	U ₁ , %	V ₁ , %/°C	T ₂ , °C	U* ₂ , %	V ₂ , %/°C	T ₃ , °C	U* ₃ , %	(U ₃ -U ₂) or (U ₃ -U ₁), %	V ₃ , %/°C
1	33.8	32	1.8	0.144	50	4.7	0.178	122	9.4	4.7	0.006
2	36.9	38	2.2	0.109	62	2.3	0.079	166	6.6	4.3	0.009
3	31.8	34	2.3	0.147				116	6.0	3.7	0.122
4	34.6	39	0.3	0.032	70	1.3	0.052	115	3.3	2.0	0.008
5	32.6	40	3.0	0.121				91	5.9	2.9	0.015
6	40.0	41	0.7	0.053	51	1.3	0.067	163	5.4	4.1	0.005

Table 4. Thermal characteristics of feathers at temperatures above 180 °C using TGA.

Sample number	U ₃ , %	T, °C	U* ₁₈₀ , %	V ₁₈₀ , %/°C	T, °C	U* ₂₀₀ , %	V ₂₀₀ , %/°C	T, °C	U* ₂₁₅ , %	V ₂₁₅ , %/°C	U ₂₁₅ -U ₃ , %
1	9.4	180	9.8	0.010	200	10.0	0.017	215	10.3	0.024	0.9
2	6.6		6.6	0.007		6.8	0.019		7.2	0.035	0.6
3	6.0		8.2	0.008		8.4	0.013		8.7	0.022	0.5
4	3.3		5.7	0.009		6.0	0.021		6.5	0.042	0.8
5	5.9		6.8	0.019		7.2	0.029		7.8	0.053	1.0
6	5.4		6.8	0.012		7.2	0.028		7.8	0.067	2.4

Then at a temperature of 115-163 (T₃), the rate of water release is significantly decreased. This step can be related to the loss of water bound in the feather structure. For each type of feather, the level of this temperature is slightly different (**Table 3**). According to work [3], in the temperature range 25-235 °C, there is a loss of free water and water bound in the feather structure.

The next stage of decomposition begins at a temperature above 150 °C. On the DTG curve an increase in the rate of mass loss is observed. Because the interpretation of further phenomena is difficult, the loss of mass at selected temperatures 180, 200 and 215 °C (U₁₈₀, U₂₀₀, U₂₁₅) and the rate of mass changes at these temperatures V₁₈₀, V₂₀₀ and V₂₁₅ were determined, respectively, results of which are summarised in **Table 4**.

The rate of mass change for the feathers tested varies r from 0.007-0.019%/°C at a temperature of 180 °C, while at 200 °C it ranges from 0.013-0.029%/°C, and at 215 °C fluctuates in the range of 0.022-0.067%/°C. The mass loss at 180 °C was 5.7-9.8%, at 200 °C – 6.0-10%, and at 215 °C it was 6.5-10.3%.

Feathers for the study came from various slaughterhouses, hence the differences (about 4%) in the total amount of degradation products released between individual feather samples.

According to Martinez – Heranandez [3], the next stage of fibre degradation begins at a temperature of about 220 °C, with a mass loss of approx. 10%. This step is associated with the disintegration of disulphide bonds and peptides.

The beginning of this stage can be associated with an endothermic peak on DSC thermograms which starts at a temperature above 150 °C (T_{end}) (**Figure 4**), the process of which is related to the melting of α-keratin.

For interpretation of DSC thermograms, the data presented in **Figure 5** were used. The DSC thermograms show a distinct endothermic peak with extreme temperature – T_m and the enthalpy of transformation – ΔH_m, and some of the samples reveal typical glass transition with the temperature – T_g. Results of the thermogram analysis are summarised in **Table 4**.

The endothermic peak on the thermogram refers to the evaporation of water bound in the keratin structure. The largest effect associated with water evaporation was observed for sample 1. The extreme

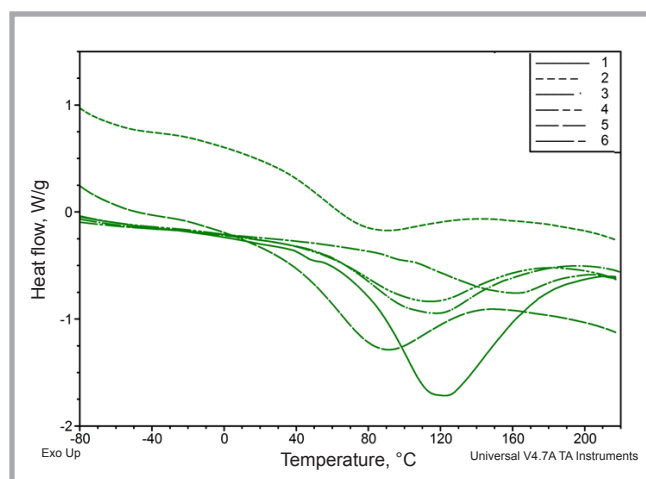


Figure 4. DSC thermograms of feather samples.

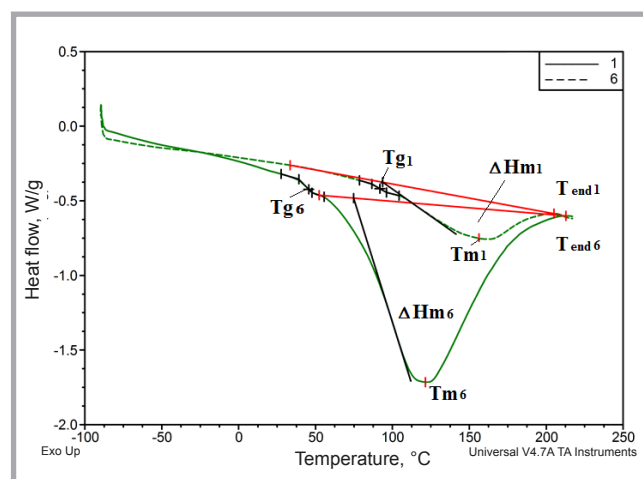


Figure 5. Presentation of the characteristic temperature of the feathers on DSC thermograms.

Table 5. Thermal characteristics of feathers using DSC.

Sample number	T _m , °C	ΔH _m , J/g	T _{end} , °C	T _g , °C
1	121.5	476	215	46
2	81.0	157	153	–
3	114.9	260	201	97
4	110.6	119	183	–
5	87.0	251	150	–
6	156.5	92	207	92

Table 6. Description of bands appearing on FTIR spectra of feathers [6].

Wave length, cm ⁻¹	Type of bond	Type of vibration
475	S-S	Symmetrical stretching
685	C-S	Symmetrical stretching
980	C-C	Symmetrical stretching
1075	C-C	Symmetrical stretching
1170	C-C	Symmetrical stretching
1230	(CN) Amide III	Symmetrical stretching
1315	CH ₂	Symmetrical bending
1385	CH ₃	Symmetrical bending
1436	CH ₃	Symmetrical bending
1455	CH ₃	–
1530	(NH) Amide II β-sheets	Symmetrical bending
1655	(C-O) Amide I α-helix,	Symmetrical stretching
1666	(C-O) Amide I β-sheets	Symmetrical stretching
1680	C-O	Symmetrical stretching
2870	CH ₂	Symmetrical stretching
2930	CH ₃	Symmetrical stretching
2965	CH ₃	Anti-symmetrical stretching
3070	NH Amide B	Anti-symmetrical stretching
3300	NH Amide A α-helix	Symmetrical stretching

Table 7. FTIR bands of feather samples tested.

Band	Wavelength, cm ⁻¹					
	1	2	3	4	5	6
S-S						455
	517		515			
	577	553		547	544	612
					671	647
C-S		700	700	697		
		927	930	927	933	921
C-C	1039		1033			
C-C	1074	1065	1080	1071	1074	1077
C-C		1154		1157	1151	1159
C-C	1168		1174			
(CN) Amide III	1233	1233	1236	1230	1227	1236
CH ₂		1316	1318	1310	1307	
CH ₂		1342	1342	1339	1342	
CH ₃		1389		1389	1386	1383
CH ₃	1404		1401			
CH ₃						
CH ₃	1448	1448	1442	1442	1448	1448
(NH) Amide II β-sheets		1516	1513	1516	1513	1513
	1525					
	1625	1627	1619	1627	1627	
(C-O) Amide I β-sheets						1640
CH ₂	2846	2846	2846	2846	2849	
CH ₂	2870	2866	2876	2870	2872	2870
CH ₃	2914	2920	2920	2920	2914	
CH ₃					2926	2929
CH ₃	2955	2958	2958	2958	2955	2960
CH ₃						
NH Amide B	3076	3070	3067	3067	3070	3067
NH Amide A α-helix	3270	3267	3267	3270	3267	3273
NH bound with hydrogen bond with C = O group	3497		3494		3505	3510

temperature of this peak is different for each of the feather samples and varies within the range of 81-157 °C. The end of this peak (T_{end}) begins the next stage, which, according to literature, refers to the melting of α-keratin [4]. For samples 1 and 6, this temperature is 215 and 207 °C, respectively. For SADA samples the temperature differs depending on the preparation method of these materials and is 201, 183 and 207 °C, respectively (**Table 5**).

Differences in the endothermic peak characteristics that are associated with the release of water bound in the α-keratin structure can be caused by variations in the structure of different fibres and/or differences in the method of their treatment.

According to Feughelman [5], α-keratin occurs in a crystalline and cross-linked form. Barone and Schmidt [1] found that bound water forms a third phase which is linked with keratin by hydrogen bonds. The treatment of fibres and their structure may affect changes in the structure of this phase.

FTIR spectra of the feathers studied are characterised by the presence of all the bands described in **Table 6**. In the range 3600-3200 cm⁻¹ there are bands associated with NH groups. Bands in the range of 3000-2800 cm⁻¹ derive from the vibrations of methylene groups.

The peak at 1645 cm⁻¹ is associated with the stretching vibrations of the carbonyl groups of amide band I, which indicates a β-type structure. The peak at 1545 cm⁻¹ is associated with the bending vibrations of the N-H group and stretching vibrations of the C-H group.

The peak at 1227 cm⁻¹ is related to amide III with stretching vibrations of the C-N group and bending vibrations of N-H groups. A strong peak at 1024 cm⁻¹ indicates a high content of residual cysteine – S-sulfonated.

Table 7 presents a list of bands appearing on the spectra of the feather samples tested, **Table 8** shows the vibration bands of the carbonyl groups of amide I, amide II, amide III and amide A & B.

Spectra distribution was carried out for spectral bands, and on this basis the content of individual structures in the samples analysed was calculated, the results

of which are presented in **Table 9**. The results were compared to those presented in the Nuutinen publication [7].

Feathers tested by Nuttinen contained 4-22% α -helix structures, 16-35% β -sheet structures, 9-17% screw structures and 42-53% rolled-coil structures. However, the samples tested in this work contained 11-25% α -helix structures, 15-40% β -sheet structures, 11-24% screw structures and 39-49% rolled-coil structures. Analysing the results of the research, it can be concluded that both groups of materials have a similar chemical structure; however, the samples differ among themselves (**Table 9**).

Detailed analysis of the chemical structure using FTIR did not explain why in some of the samples melting of the α -helical structure begins at a temperature of about 150 °C, which is why TGA-IR analysis was also performed. **Figures 6-10** show spectra of the gaseous degradation products of feather samples after exposure at various temperatures, and **Figure 11** presents temperatures at which gas products were analysed for selected sample no 6.

For sample 5, due to the over-fragmentation of feathers, the gaseous degradation products could not be determined. The FTIR spectra (**Figures 6-10**) reveal bands originating from vibrations of water compounds, CO₂, containing oxygen groups C-O and C-OH.

At 32 °C no bands from the gaseous products were detected, and at 70 °C the occurrence of bands related to vibrations of water molecules was observed. At 150 °C, no bands from gaseous products were observed, and at a temperature of 225 °C there are bands with low intensity originating from compounds containing oxygen groups C-O and C-OH in the range of 1336-1375 cm⁻¹ and 920-960 cm⁻¹.

At 257 °C, bands originating from vibrations of water compounds, CO₂, containing oxygen groups C-O and C-OH appear; however, these may be products of the degradation of keratin (**Figure 11**).

The kinetics of the gas emission process during the analysis using TGA-IR are shown in **Figures 12-17**.

The analysis of the kinetics of the gas emission process during the decomposition of keratin indicates that at the initial stage of degradation at a temperature up

Table 8. FTIR bands of amide origin

Sample number	Band	Wavelength, cm ⁻¹			
		α -helix	β -sheets	Screw structure	Rolled coil
1	Amide I		1625		
	Amide II			1516	
	Amide III				1233
	Amide A	3076			
	Amide B	3270			
2	Amide I		1627		
	Amide II			1516	
	Amide III				1233
	Amide A	3070			
	Amide B	3267			
3	Amide I		1619		
	Amide II			1513	
	Amide III				1236
	Amide A	3067			
	Amide B	3267			
4	Amide I		1627		
	Amide II			1516	
	Amide III				1230
	Amide A	3067			
	Amide B	3270			
5	Amide I		1627		
	Amide II			1513	
	Amide III				1227
	Amide A	3070			
	Amide B	3267			
6	Amide I		1640		
	Amide II			1513	
	Amide III				1236
	Amide A	3067			
	Amide B	3273			

Table 9. Content of individual structures in the feathers.

Sample number	α -helix, %	β -sheet, %	Screw structure, %	Rolled-coil, %
1	22.2	20.6	12.1	45.0
2	25.3	14.9	17.7	42.1
3	14.9	25.5	11.2	48.3
4	18.9	18.1	23.8	39.2
5	11.3	25.3	15.7	47.7
6	—	39.8	10.9	49.3

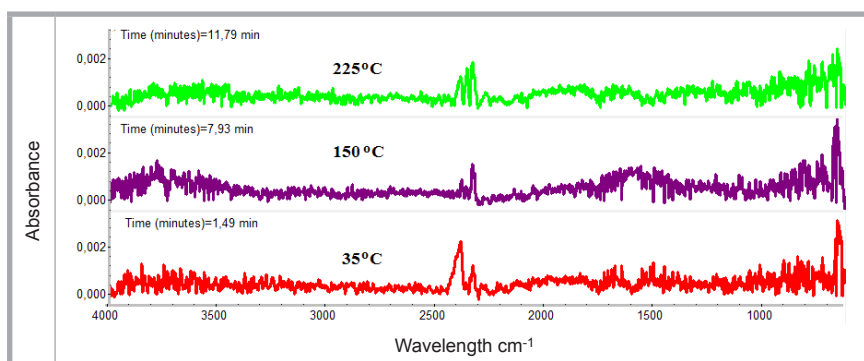


Figure 6. Spectra of gaseous degradation products of sample 1 after exposure at different temperatures.

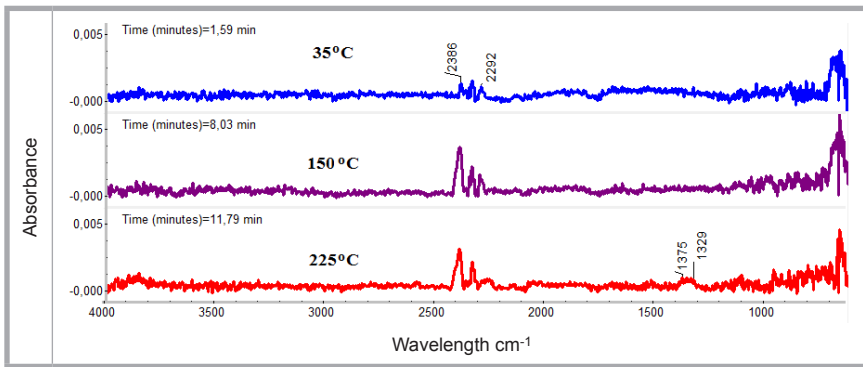


Figure 7. Spectra of gaseous degradation products of sample 2 after exposure at different temperatures.

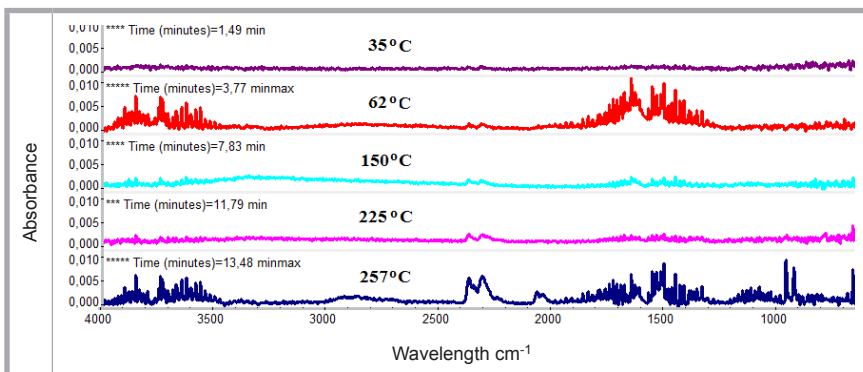


Figure 8. Spectra of gaseous degradation products of sample 3 after exposure at different temperatures.

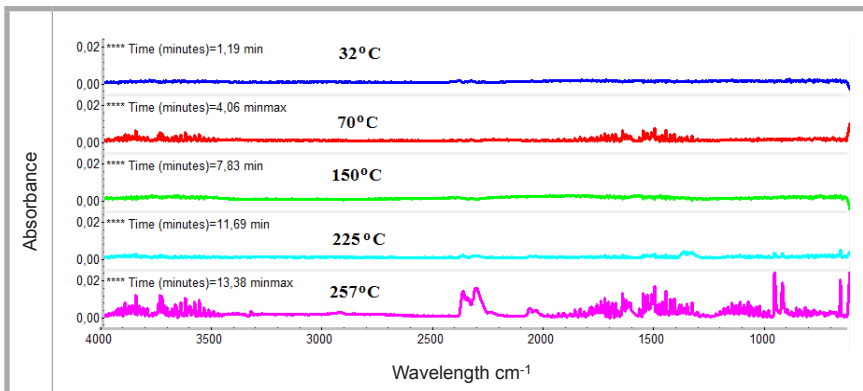


Figure 9. Spectra of gaseous degradation products of sample 4 after exposure at different temperatures.

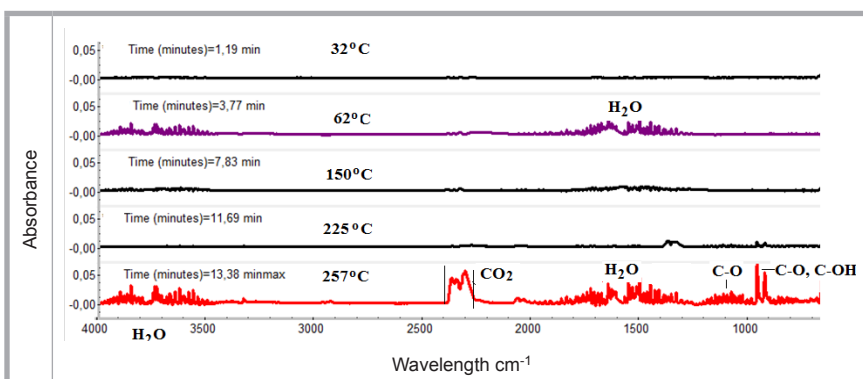


Figure 10. Spectra of gaseous degradation products of sample 6 after exposure at different temperatures.

to about 150 °C, water is released from the samples.

According to Staroń [8], the process of keratin degradation under the influence of elevated temperature leads to the formation of oligomers, polypeptides and amino acids, and noticeable changes are already observed after heating at 185 °C for 30 s. These observations confirm the results of research conducted within the work. On the FTIR spectra of decomposition products at temperatures above 180 °C, bands indicating the release of gases other than water and carbon dioxide appear, as indicated by the bands at 2930-2960 cm^{-1} and 900-1200 cm^{-1} .

As a result of the tests, it was found that the temperature of the beginning of the melting of α - helix structures vary for the samples tested. These differences may be due to variations in the structure of feathers and/or in the method of their treatment.

In the case of analysis using TGA/IR, it was found that at a temperature up to 150 °C water is released from the feathers. The amount of volatile products released at this temperature among the samples analyzed varies by about 4%. When testing samples using FTIR, TGA, DSC and TGA / IR techniques, no differences in fat content were observed.

On the basis of the results obtained, a temperature 190 °C of the formation process of fibrous composites with the addition of feathers was determined. In order to ensure a correct interpretation of results regarding the thermal stability of keratin fibres in feathers, a spun bonded nonwoven with the addition of shredded feathers was formed, from which thermoset composites were made. For selected samples of spun-bonded nonwoven and thermoset composites, TG-DSC analysis was performed.

Analysis of nonwovens and composites with keratin addition

In the case of nonwoven PP and PP/4% CF, the following endothermic peaks were observed: for PP at a temperature of 173 °C and for PP/4% CF at 172 °C. They most probably correspond to the melting of PP (**Figure 18**).

For composites KMC-1 and KMC-2 (+ 4% CF), we can observe two endothermic peaks on the DSC curve. The first is

in the range of lower temperatures with a maximum at a temperature of 58 °C for the composite with PP and at 55 °C for composite PP + 4% CF, and the second is in the range of higher temperatures, with a maximum at 174 °C for the PP composite and 172 °C for composite PP + 4% CF (Figure 19).

For PLA non-woven samples, we can observe peaks at lower temperatures: an endothermic peak at 68.2 °C, being an overlapping of the specific heat at PLA glass transition and the endothermic effect of stress relaxation, as well as an exother-

Figure 11. TGA and DTG thermogram with marked temperatures at which gas products were analysed for sample 6.

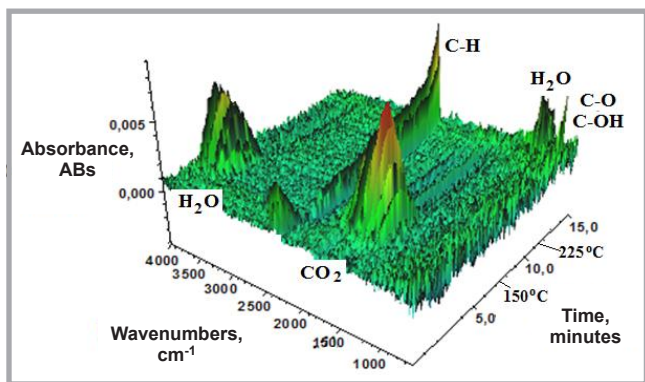
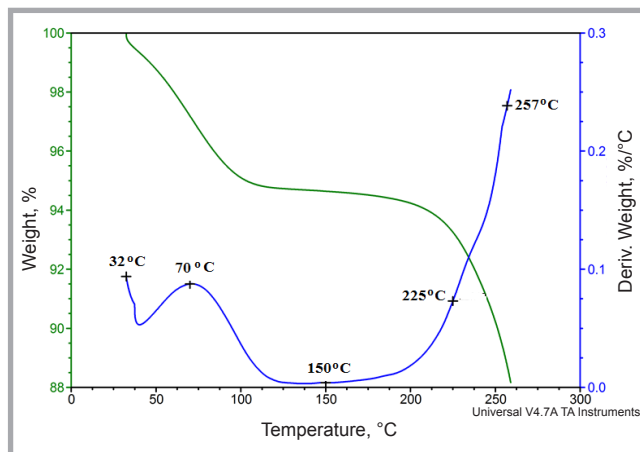


Figure 12. 3D image of the results of kinetics analysis of the gas emission process for sample 1.

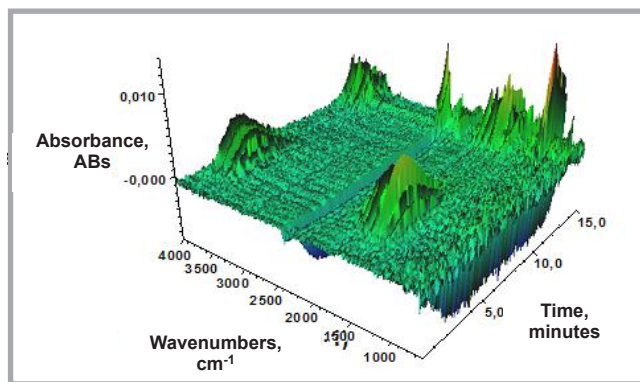


Figure 13. 3D image of the results of kinetics analysis of the gas evolution process for sample 2.

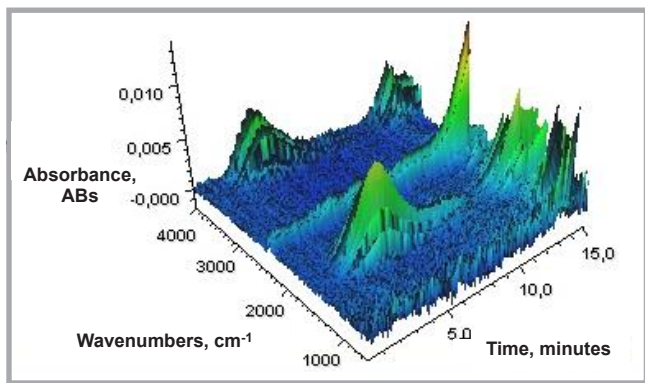


Figure 14. 3D image of the results of kinetics analysis of the gas evolution process for sample 3.

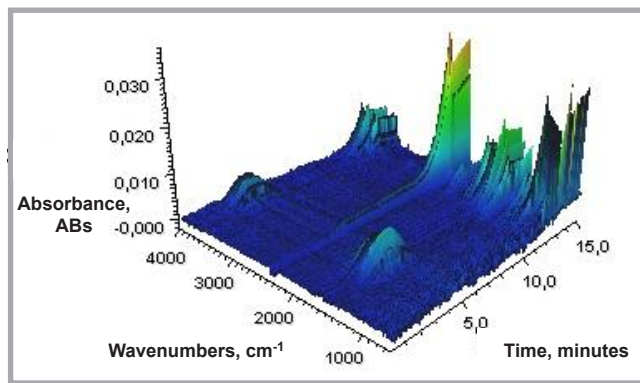


Figure 15. 3D image of the results of kinetics analysis of the gas evolution process for sample 4.

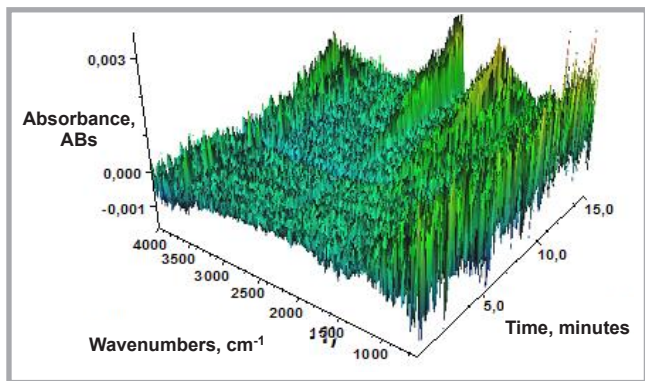


Figure 16. 3D image of the results of kinetics analysis of the gas evolution process for sample 5.

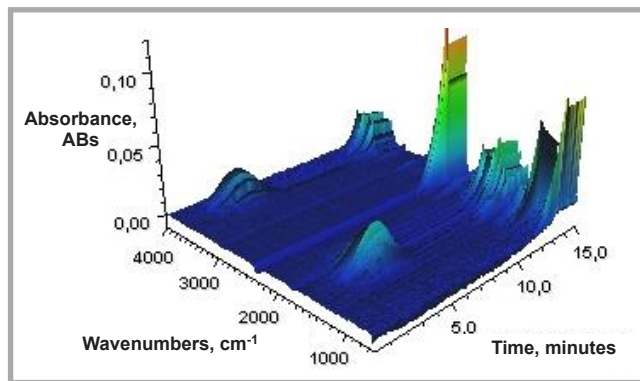


Figure 17. 3D image of the results of kinetics analysis of the gas evolution process for sample 6.

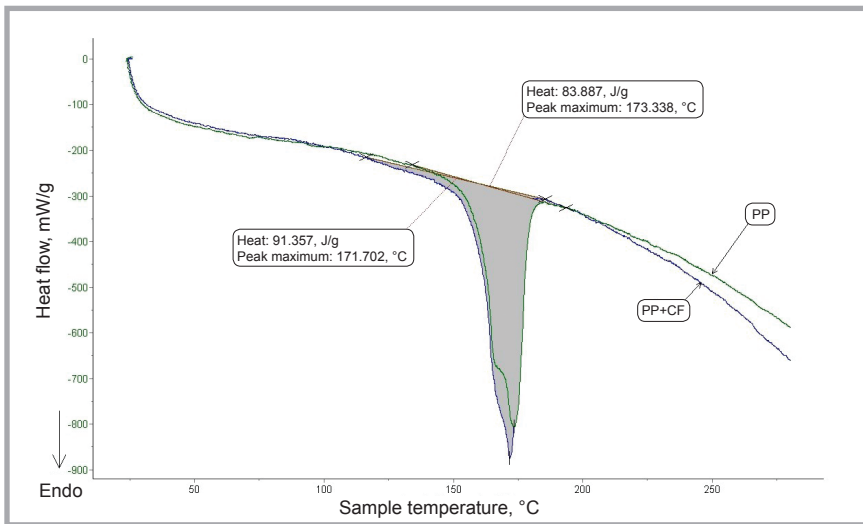


Figure 18. DSC thermograms for spun-bonded nonwoven PP and PP/CF.

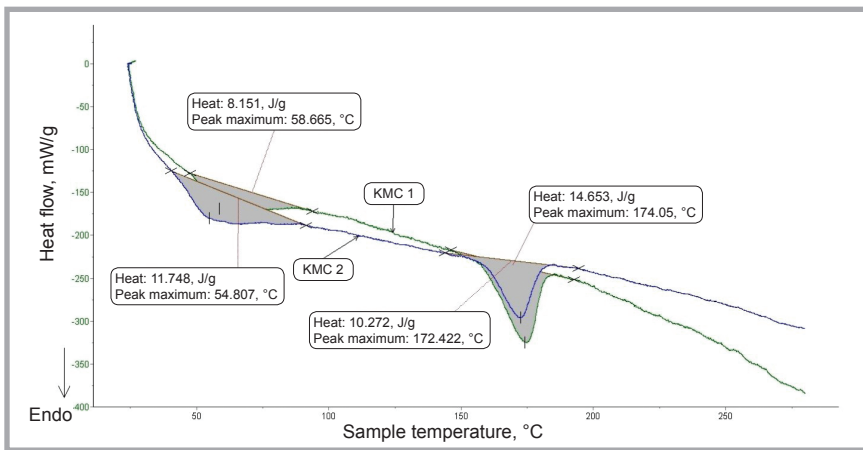


Figure 19. DSC thermograms for thermoset composites PP and PP/CF.

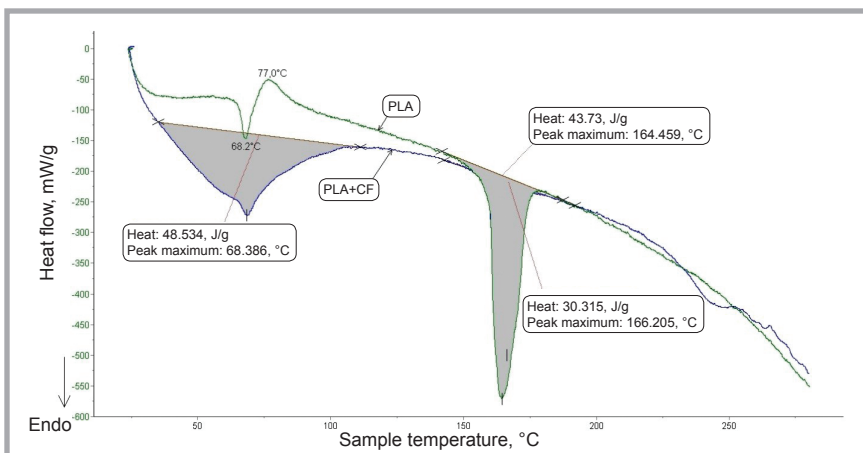


Figure 20. DSC thermograms for spun-bonded nonwoven PLA, PLA/CF.

Table 10. Mechanical properties of PP and PLA based non-woven thermoset composites. Note: *5 layers in all composites.

Thermoset composite	Non-woven*	Young's modulus, MPa	Tensile strength, MPa	Elongation at break, %
KMC-1	PP	1365 ± 216	33.7 ± 3.3	6.0 ± 1.8
KMC-2	PP+CF	1385 ± 103	26.5 ± 0.8	5.2 ± 0.4
KMC-3	PLA	1733 ± 121	32.6 ± 1.8	2.8 ± 0.3
KMC-4	PLA+CF	1634 ± 188	36.5 ± 3.4	3.4 ± 0.6

mic peak at 77.0 °C, most likely associated with the cold crystallisation effect of PLA.

For non-woven PLA/CF in the range of lower temperatures, there may be similar effects to those of the above-mentioned PLA non-woven, but there appears an additional, much stronger, endothermic effect most likely associated with the evaporation of water from the keratin component.

For both samples, a second peak is observed in a range of higher temperatures, with the maximum at 166 °C for PLA/CF and 164 °C for PLA non-woven, associated with the endothermic melting effect of PLA

For thermoset composites PLA and PLA/CF, we can also observe two peaks, one in the lower range and the other in the higher temperature range, respectively:

- for PLA (KMC-3) composite: 59 °C and 163 °C
- for PLA/CF (KMC-4) composite: 61 °C and 164 °C

Analysing DSC curves for both PP & PLA spun-bonded nonwoven (Figures 18 and 20) and PP & PLA thermoset composites with or without feathers additions (Figures 19 and 21), temperature differences between the individual peaks are so small that it is difficult to conclude unambiguously about the influence of the keratin component and other parameters (composition of nonwoven and composites) on the thermal properties of end products.

For selected thermoset composites the mechanical properties were determined, illustrated in Table 10.

Assessment of the mechanical properties showed a decrease in the mechanical properties of PP based non-woven composites with the incorporation of feathers, while a notable improvement in the tensile strength and elongation at break of PLA based non-woven composites was observed with the addition of feathers (Table 10). In the first case, the lower tensile strength for the PP/CF nonwoven based composite could be attributed to the low wettability of resin. In the case of PLA/CF the presence of a high amount of feathers seems to have a big influence on the tensile strength of the composite, attributed to high resin absorption by the feathers. However, further investigation

is necessary to assess in detail the absorption of resin by each type of fabric.

FE-SEM images (**Figures 22, 23**) show that in all cases PP and PLA fibres are not totally embedded in the thermoset resin. The presence of feathers was also corroborated, showing a higher amount of feathers in PLA-based non-wovens in comparison with PP-based non-woven.

Conclusions

- Investigations of the thermal properties of keratin fibres contained in feathers are very important from the point of view of their further processing into feather-based products, such as keratin-containing nonwovens and composites.
- Knowledge of the thermal properties of keratin fibres in feathers allowed to determine the parameters of their processing without fear of degradation of the keratin structure.
- Found was the possibility of forming PP and PLA nonwovens and thermoset composites with the addition of keratin fibres at the flow temperature of the base polymer i.e. 190-210 °C, respectively.
- PP and PLA based nonwovens with and without feathers were successfully used for the preparation of bio-based thermoset composites with good mechanical properties. PLA/CF nonwoven based composites showed higher tensile strength than only PLA based nonwoven composites. This increase in the tensile strength may be attributed to the high feather content of PLA/CF nonwoven, which could increase resin absorption in the composite.

Acknowledgements



The investigation presented in this paper was carried out as part of research project KaRMA2020. This project has received funding from the European Union's Horizon 2020 Research and Innovation program under Grant Agreement No. 723268.



References

- Barone JR, Schmidt WF. Effect of formic acid exposure on keratin fiber derived from poultry feather biomass. *Bioresource Technology* 2006, 97, 233- 242.
- Cardamone JM. Investigating the microstructure of keratin extracted from wool: Peptide sequence (MALDI-TOF/TOF) and protein conformation (FTIR). *Journal of Molecular Structure* 2010, 969, 97-105.
- Martínez-Hernández L, Velasco-Santos C, de Icaza M, Castaño V M. Grafting of methyl methacrylate onto natural keratin. *e-Polymers* 2003, no. 016.
- Schmidt WF, Line, MJ. Physical and Chemical Structures of Poultry Feather Fiber Fraction in Fiber Process Development. In: *Proceedings of the TAPPI Nonwovens Conference 1996 March 11-13*; Charlotte, NC. Atlanta, GA: Technical Association of the Pulp and Paper Industry, 1996; pp.135-140.
- Feughelman M. *Mechanical Properties and Structure of Alphakeratin Fibres*. University of New South Wales Press, Sydney 1997; 24-27.
- Tesfaye T, Sithole B, Ramjugernath D. *Sustainable Chemistry and Pharmacy* 2018; 8: 38-49.
- Nuutinen EM. *Feather characterization and processing*. Aalto University 2017.
- Staroń P, Banach M, Kowalski Z. *Chemia* 2011; 65, 10: 1019-1026.

Received 07.03.2019 Reviewed 13.05.2019

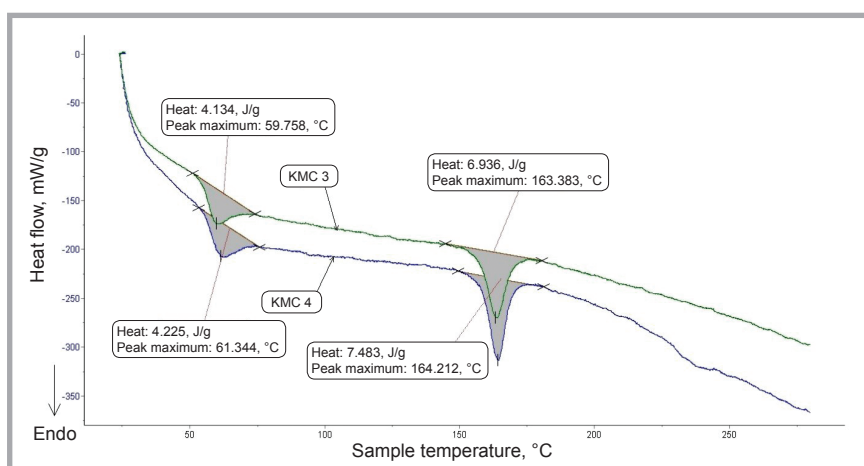


Figure 21. DSC thermograms for spun-bonded nonwoven PLA, PLA/CF.

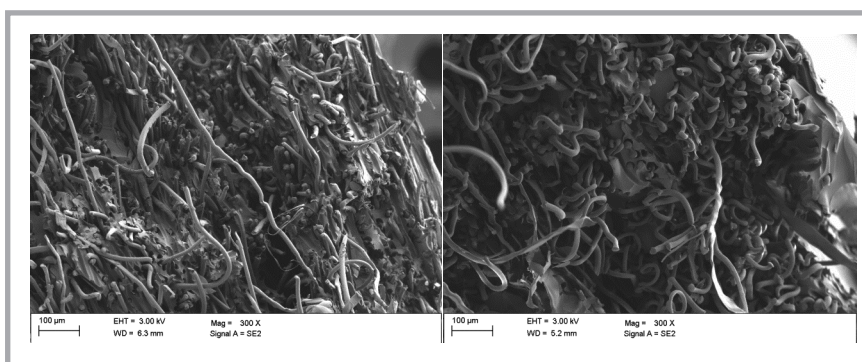


Figure 22. FM SEM photo of thermoset composites based on PLA and PP nonwoven.

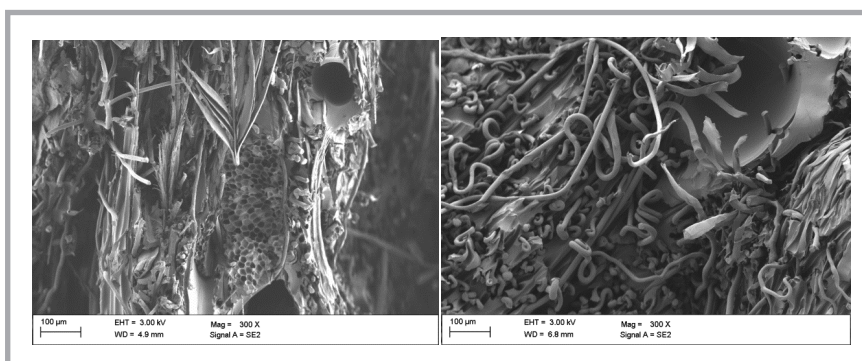


Figure 23. FM SEM photo of thermoset composites based on PLA/CF and PP/CF nonwoven.